Development 139, 760-771 (2012) doi:10.1242/dev.074104

A putative tyrosine phosphorylation site of the cell surface receptor Golden goal is involved in synaptic layer selection in the visual system

Klaudiusz Mann, Mengzhe Wang, Si-Hong Luu, Stephan Ohler, Satoko Hakeda-Suzuki and Takashi Suzuki*

SUMMARY

Golden goal (Gogo) is a cell surface protein that is crucial for proper synaptic layer targeting of photoreceptors (R cells) in the *Drosophila* visual system. In collaboration with the seven-transmembrane cadherin Flamingo (Fmi), Gogo mediates both temporary and final layer targeting of R-cell axons through its cytoplasmic activity. However, it is not known how Gogo activity is regulated. Here, we show that a conserved Tyr-Tyr-Asp (YYD) tripeptide motif in the Gogo cytoplasmic domain is required for photoreceptor axon targeting. Deleting the YYD motif is sufficient to abolish Gogo function. We demonstrate that the YYD motif is a phosphorylation site and that mutations in the YYD tripeptide impair synaptic layer targeting. Gogo phosphorylation results in axon stopping at the temporary targeting layer, and dephosphorylation is crucial for final layer targeting in collaboration with Fmi. Therefore, both temporary and final layer targeting strongly depend on the Gogo phosphorylation status. *Drosophila* Insulin-like receptor (DInR) has been reported to regulate the wiring of photoreceptors. We show that insulin signaling is a positive regulator, directly or indirectly, of YYD motif phosphorylation. Our findings indicate a novel mechanism for the regulation of Gogo activity by insulin signaling-mediated phosphorylation. We propose the model that a constant phosphorylation signal is antagonized by a presumably temporal dephosphorylation signal, which creates a permissive signal that controls developmental timing in axon targeting.

KEY WORDS: Gogo, Tyrosine phosphorylation, Axon guidance, *Drosophila*

INTRODUCTION

The parallel organization of synaptic layers (laminae) is widely observed in vertebrate and invertebrate brains. How neuronal cells find specific synaptic targets to achieve a stereotyped pattern of connections is one of the central questions in neurobiology (Sanes and Zipursky, 2010). The *Drosophila* compound eye comprises 750 simple eyes, each containing eight photoreceptor neurons (R1-R8, Fig. 1A-C). The R1-R6 neurons innervate the first optic neuropile, termed the lamina, whereas R7 and R8 neurons form connections in the second ganglion, the medulla [the M6 and M3 layers, respectively (Clandinin and Zipursky, 2002)]. The R8 axon targeting occurs in a stepwise fashion (Fig. 1B) (Ting et al., 2005). In the first step, R8 axons reach the temporary layer in the medulla by 24 hours after pupa formation (APF) and pause there. The second step starts after 50 APF, when the R8 growth cones project to a deeper layer, which later becomes the R8 recipient layer (M3).

In *Drosophila*, three cell surface molecules have been implicated in R8 photoreceptor targeting: Capricious (Shinza-Kameda et al., 2006), the seven-transmembrane cadherin Flamingo (Fmi; Starry Night – FlyBase) (Lee et al., 2003; Senti et al., 2003) and Golden goal (Gogo) (Tomasi et al., 2008; Hakeda-Suzuki et al., 2011). Gogo and Fmi participate in both temporary and final layer targeting. Gogo contributes to anchoring R8 axons in their temporary layer and is necessary for axon extension to the final target layer in the mid-pupa (Tomasi et al., 2008; Hakeda-Suzuki et al., 2011). How does Gogo regulate these sequential targeting steps?

Several studies have led to the view that tyrosine phosphorylation plays a role in axon guidance and target recognition; examples include the tyrosine kinases [Eph (Henkemeyer et al., 1996), Derailed (Callahan et al., 1995), Src family (Knoll and Drescher, 2004), Alk (Bazigou et al., 2007), Robo and Abl (Bashaw et al., 2000)] and phosphatases [Lar and Ptp69D (Clandinin et al., 2001; Maurel-Zaffran et al., 2001)].

The *Drosophila* Insulin-like receptor (DInR) is a tyrosine kinase that has been reported to regulate the wiring of photoreceptors (Song et al., 2003). DInR binds to Dock and triggers the Dock/Pak pathway (Garrity et al., 1996; Hing et al., 1999). DInR is enriched in R-cell projections and axons mutant for *dinr* (*InR* – FlyBase) fail to reach their targets (Song et al., 2003). The ligands of DInR, insulin-like peptides (DILPs), are secreted into the circulatory system (Rulifson et al., 2002). Therefore, insulin signaling is unlikely to provide a directional cue for axonal growth cones and the exact mechanism of insulin signaling in retinal axon targeting remains unclear.

We previously found that the Gogo protein has a conserved YYD tripeptide motif in the cytoplasmic domain (Tomasi et al., 2008). Here, we show that this motif is a tyrosine phosphorylation site and is essential for Gogo function. DInR positively regulates Gogo phosphorylation in a direct or indirect manner, and phosphorylated Gogo enhances the adhesion of R8 axons to the M1 layer. Moreover, the phosphorylation status of Gogo is critical for its collaboration with Fmi to recognize the M3 layer during the final targeting of R8 cells. Therefore, mechanisms regulating the gogo phosphorylation status can contribute to the fine-tuning of retinal axon targeting.

Max Planck Institute of Neurobiology, Am Klopferspitz 18, D-82152 Martinsried, Germany.

*Author for correspondence (suzukit@neuro.mpg.de)

Accepted 9 December 2011

MATERIALS AND METHODS

Animals and molecular cloning

Flies were kept in standard *Drosophila* medium at 25°C, except for the co-overexpression of *gogo* and *fmi* (20°C). The following fly stocks and mutant alleles were used: *gogo[H1675]*, *UAS-gogo T1, Rh4-mCD8-4xGFP-3xmyc* (abbreviated as *Rh4-GFP*), *Rh6-mCD8-4xGFP-3xmyc* (abbreviated as *Rh6-GFP*), *ey*FLP2 (Newsome et al., 2000), *ey3.5*FLP; 3L *cl FRT80*/TM6B*y*+ and *ato-tau-myc* (I. Salecker, NIMR, London, UK), *GMR-mCD8-mKO-myc*, *yw; GMR-Gal4*, *yw ey*FLP2; *FRT82B GMR-mCD8-KO*/TM6, *yw*; *P{UAS-InR.K1409A}*2 (Bloomington), *yw; P{UAS-InR.A1325D}*2 (Bloomington), *FRT82B dinr*^{ex15}/TM3 (Song et al., 2003), *yw, dilp6*^{68}*; dilp1-4*^{1}*, 5*^{4}*/TM3Sb* (Gronke et al., 2010), *w; UAS-fmi-P40*, *w; GMR-gogoC1-myc T1*, *w; GMR-gogoC2-myc T2a*, *w; GMR-gogoC3-myc T3b*, *w; GMR-gogoC1C2-myc T2*, *w; GMR-gogoC2C3-myc T2*, *w; GMR-gogoC1C3-myc T1*, *w; GMR-gogoC1C3-myc T2*, *w; GMR-gogoFL-P40*, *w; GMR-gogoFFD T4a*, *GMR-gogoFYD-P40*, *w; GMR-gogoYFD-P40*, *w; GMR-gogoDDD-P40*, *w; GMR-gogoΔYYD-P40*, *w; GMR-gogoYDD-P40*, *w; GMR-gogoDYD-P40*, *w; GMR-gogoC2*^{shortFFD}*-P40*, *w; UAS-gogoFL-P40*, *w; UAS-gogoFFD-P40*, *UAS-gogoFYD-P40*, *w; UAS-gogoYFD-P40*, *w; UAS-gogoDDD-P40*, *w; UAS-gogoΔYYD-P40*, *w; UAS-gogoYDD-P40*, *w; UAS-gogoDYD-P40*.

For PhiC31 integrase-mediated transgenesis (P40), transgenes were incorporated into the *yv; P{nos-phiC31\int.NLS}X; P{CaryP}attP40* (Bloomington) (Bischof et al., 2007) background by BestGene. Insertions were confirmed by PCR using primers pCARYP_1 (5′-CTCGAGGGGATCCCCCTAGTACTGACGGA-3′) and attB1 (5′-GGAAGAGCGCCCAATACGCAAACCGCCTCT-3′).

For biochemistry the following constructs were used: *UAS-gogo-myc*, *UAS-gogo*^{9F}*-myc*, *UAS-gogoC2*$^{short\ FFD}$*-myc*, *UAS-gogoC2*$^{short\ FYD}$*-myc*, *UAS-gogoC2*$^{short\ YFD}$*-myc*, *UAS-gogoC2*$^{short\ YYD\ FFF}$*-myc*. The *UAS-dinr-GFP* construct was generated with the Gateway System (Invitrogen) using the pENTR-InR vector (E. Hafen, ETH Zürich).

Immunochemistry, imaging and assessment of R8 photoreceptor phenotypes

Immunostaining of eye-brain complexes was performed as described (Wu and Luo, 2006). Antibodies were used as described previously (Hakeda-Suzuki et al., 2011). *Rh6-GFP* was used for R8 and *Rh4-GFP* for R7 axon visualization. Mab24B10 was used to stain all photoreceptors and anti-Ncad antibody was used to stain neuropiles. Images were obtained with an Olympus FV-1000 confocal microscope and processed with Adobe Photoshop.

In Fig. 2B,C,E,G,I, Fig. 3E, Fig. 5 and Fig. 7D the number of R8 axons stopping was calculated manually as a fraction of all GFP-expressing photoreceptors. In Fig. 4 and supplementary material Fig. S4 the R8 axon stopping was clearly visible; however, as R8 axons overlapped before entering the medulla a precise quantification was not possible and we estimated the stopping, as described previously (Hakeda-Suzuki et al., 2011), by comparing the number of M3 layer innervating R8 photoreceptors between wild type and the tested sample (wild type, 3.5 axons/μm). In Fig. 6D-G, Fig. 7E,F,Q and Fig. 8A-C,E the area of the M1 blob and the diameter of R8 axons were calculated manually using the Olympus FV-1000 software.

Cell culture, biochemistry and phospho-Gogo-specific antibody

S2 cells were cultured at 25°C. All expression constructs contained the *UAS* promoter and were cotransfected with *pActin5C-Gal4* using Cellfectin (Invitrogen) or FuGENE HD Transfection Reagent (Roche). Co-immunoprecipitation, immunoblotting and aggregation assays were performed as previously described (Hakeda-Suzuki et al., 2011). All solutions used contained 2 mM Na_2VO_3 (a phosphatase inhibitor) unless stated otherwise. Prior to lysis, 2 mM Na_2VO_3 was added to the cell culture for 3 hours. We used the following antibodies: anti-Myc 9E10, 1:100 (Santa Cruz); anti-GFP JL-8, 1:3000 (Clontech); anti-phosphotyrosine 4G10, 1:2000 (Millipore). For insulin treatment, human recombinant insulin (Invitrogen) was added to the medium 20 hours prior to cell lysis. Western blots were quantified using ImageJ 1.44p.

The anti-phospho-Gogo antibody (Ab2795-D01) was generated by Peptide Institute, Japan. It was preabsorbed in 1:1 (v/v) fixed *Drosophila* embryo overnight to reduce nonspecific binding and diluted 1:250 for western blotting.

RESULTS

Gogo requires the cytoplasmic central region for its function

We have shown previously that the Gogo intracellular region is crucial for its function, as Gogo that lacks the entire cytoplasmic domain does not rescue the *gogo*$^{-}$ mutant phenotype (Tomasi et al., 2008). However, the functional elements in the Gogo cytoplasmic domain and their role in intracellular signaling are unknown. To obtain initial clues about the functional units, the cytoplasmic domain was divided into three sections: C1, C2 and C3, covering amino acids 726-953, 954-1105 and 1106-1272, respectively (Fig. 1D) (Ohler et al., 2011). Gogo expression constructs comprising the Gogo extracellular domain, the transmembrane domain (with the following 20 amino acids) and different Gogo cytoplasmic domain deletions (GogoC1, GogoC2, GogoC3, GogoC1C2, GogoC2C3, GogoC1C3) were expressed in *gogo*$^{-}$ *ey*FLP mosaic flies (eye mutant for *gogo* in an otherwise wild-type background), under the control of the photoreceptor-specific *GMR* promoter, to test their rescuing ability of the mutant phenotype (Fig. 1E-L). The *ey*FLP *gogo*$^{-}$ mutant animals display a severe phenotype, with incomplete medulla rotation and the formation of abnormal bundles through an ectopic chiasm (Fig. 1E) (Tomasi et al., 2008). This mutant phenotype is completely rescued when a transgene encoding the full-length Gogo sequence is expressed (Fig. 1F). Expression of the GogoC2 construct completely rescues the *ey*FLP *gogo*$^{-}$ mutant phenotype (Fig. 1H). By contrast, GogoC1 and GogoC3 are nonfunctional, as the *gogo*$^{-}$ phenotype is not rescued to any extent (Fig. 1G,I). Furthermore, GogoC1C2 and GogoC2C3, but not GogoC1C3, is able to rescue the *gogo*$^{-}$ phenotype (Fig. 1J-L).

These results strongly suggest that the middle region (C2) of the Gogo cytoplasmic domain includes the minimal intracellular fragment necessary and sufficient for Gogo function.

The YYD motif has a crucial function

Our bioinformatics study revealed that, although there is no overall conservation within the cytoplasmic domain, the C2 fragment contains a motif that is specific for *gogo* orthologs: a short sequence containing a highly conserved Tyr1019-Tyr1020-Asp1021, or YYD, tripeptide motif (Fig. 2A) (Tomasi et al., 2008). The conservation of the YYD motif strongly suggests that it might serve as a regulatory site and/or protein interaction domain.

To elucidate whether the YYD motif has a function in axonal pathfinding, we generated a transgenic fly line expressing full-length Gogo but lacking the YYD motif (*GMR-gogoΔYYD*). Interestingly, in contrast to wild-type Gogo, GogoΔYYD could not rescue the mutant phenotype (Fig. 2B-D), indicating that the YYD motif is indeed crucial for Gogo cytoplasmic activity.

The YYD motif is a potential phosphorylation site

Having confirmed the necessity of the YYD tripeptide for Gogo function, we sought to determine the role of these residues. Changes in the tyrosine phosphorylation of proteins are a commonly used mechanism of modulating protein activity (Maher and Pasquale, 1988; Alonso et al., 2004; Liu et al., 2004; Tarrant and Cole, 2009). Analyses of the effect of protein phosphorylation typically involve site-directed mutagenesis (Tarrant and Cole,

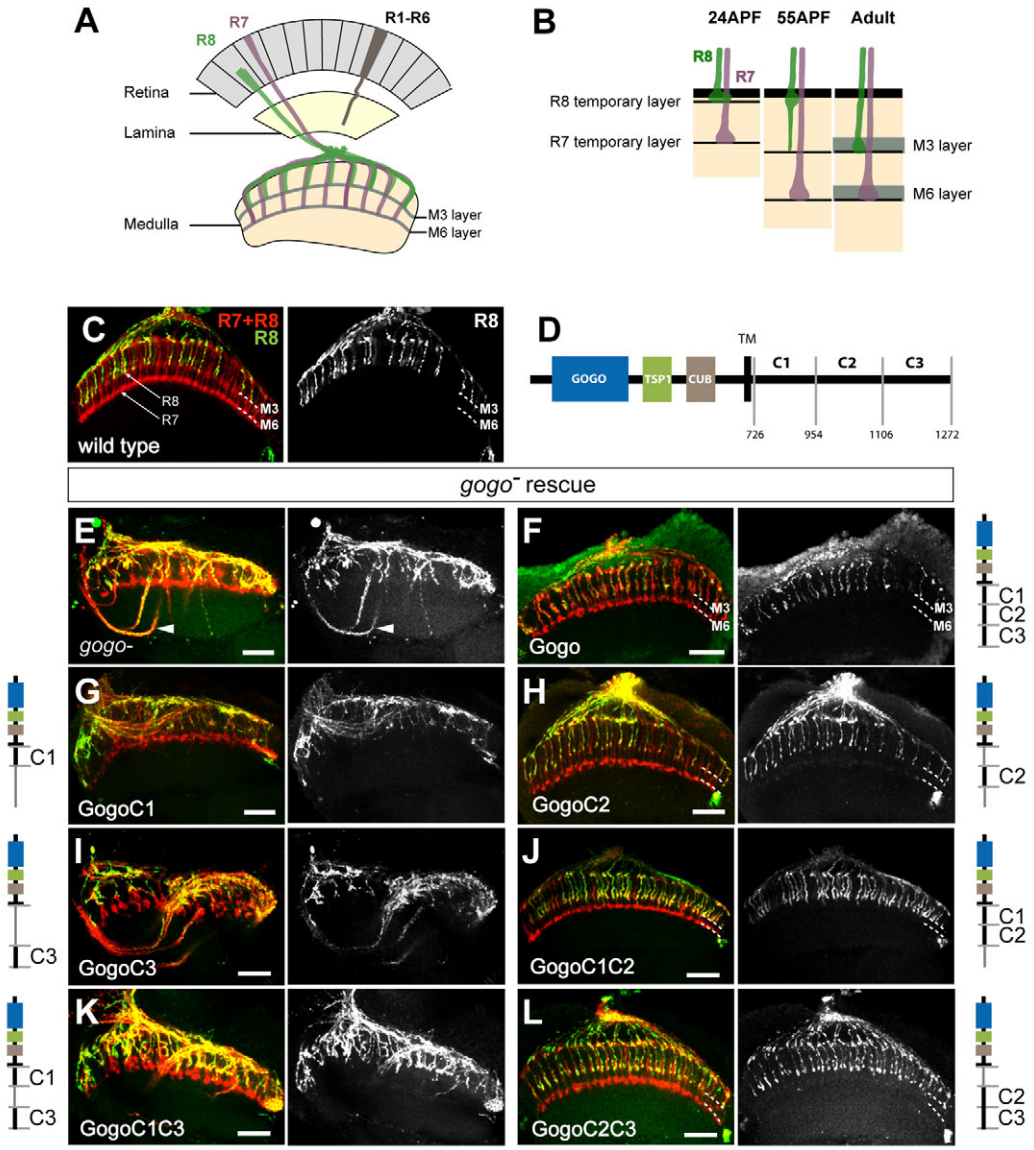

Fig. 1. Gogo requires the cytoplasmic central region for its function. (**A**) The *Drosophila* adult visual system. (**B**) In young pupae (24 APF) R7/8 axons reach their temporal layers and pause until 50 APF. Later, they start to project to the recipient layers. Neural development is completed at the end of the pupal stage. (**C**) The wild-type medulla. R8 axons target the M3 layer, whereas R7 axons target the M6 layer. Dashed lines indicate medulla layers. (**D**) Gogo protein structure. The GOGO, TSP1 and CUB domains are followed by a transmembrane domain (TM). C1, C2 and C3 sections were defined arbitrarily; the numbers indicate amino acid residues. (**E-L**) Gogo truncations (*GMR* promoter driver) were expressed in an *ey3.5*FLP *gogo*$^{-}$ mutant background. Eyes mutant for *gogo*$^{-}$ (E) show a medulla rotation defect and misguided axons (arrowhead). The *gogo*$^{-}$ mutant phenotype is rescued by full-length Gogo and by GogoC2, GogoC1C2 and GogoC2C3, but not by GogoC1, GogoC3 and GogoC1C3. Scale bars: 20 μm.

2009), in particular the replacement of tyrosine with phenylalanine (F) to mimic the unphosphorylated status (Xia et al., 2008; Tarrant and Cole, 2009). Similarly, acidic substitutions (e.g. aspartic acid, D) are useful as phosphomimetics (Tarrant and Cole, 2009; Zang et al., 2008). We examined in vivo the ability of *gogo* phosphomimetic constructs to rescue the mutant phenotype. In order to exclude the possibility that the observed phenotypes are manifested due to differences in expression levels among fly lines and not because of differences in function, we inserted all transgenes into the same locus using the PhiC31 integrase-mediated transgenesis system (Fig. 2C-J), and a similar expression level was confirmed by anti-Gogo staining (supplementary material Fig. S1A-D). The following *gogo* transgenes (driven by the *GMR* promoter) were tested: Gogo (wild type), GogoFFD (non-phospho-Gogo) and GogoDDD (phospho-Gogo). Because we did not succeed in inserting the GogoFFD transgene into the landing site locus, we used a random insertion with an expression level that was similar to that of the other transgenes (supplementary material Fig. S1D). Expression of wild-type Gogo completely rescues the mutant phenotype (*gogo*$^{-}$ *ey*FLP, Fig. 2A). Interestingly, only the non-phosphorylated GogoFFD, but not GogoDDD, is able to reconstitute the wild-type function of Gogo (Fig. 2E,F). Differences in the rescuing ability indicate that the Gogo phosphorylation status might be critical for regulating Gogo activity.

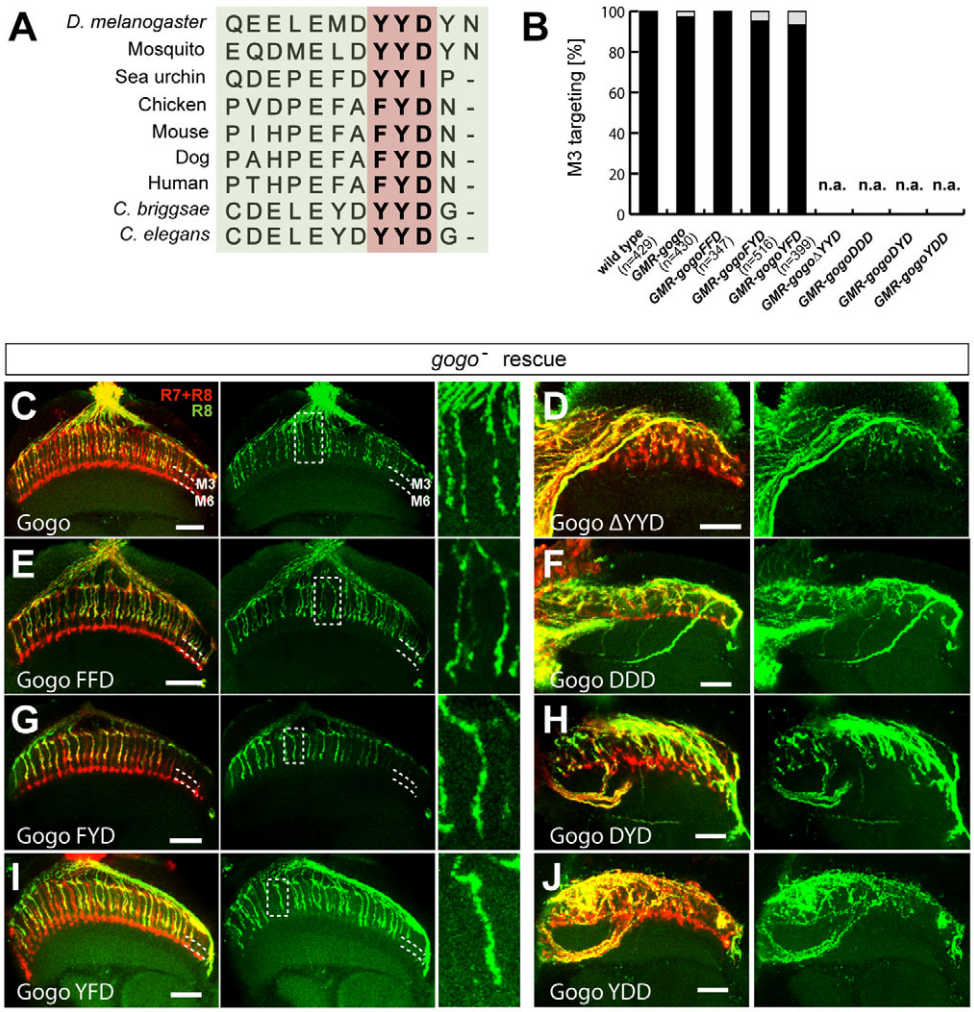

Fig. 2. The YYD motif has a crucial function. (**A**) Conservation of the YYD motif (red). (B-J) Requirement of the YYD motif. Transgenes were expressed (*GMR* promoter) in the *gogo*⁻ background (*ey3.5*FLP mosaics). (**B**) Quantification of the rescue experiments. The percentage of R8 axons targeting the M3 layer was determined. For the non-rescuing constructs, the R8 targeting could not be assessed because of the severity of the phenotype (n.a.). (**C**,**D**) The *gogo*⁻ phenotype is rescued by *GMR-gogo*, but not when the YYD tripeptide is removed (*GMR-gogoΔYYD*). (**E**,**G**,**I**) Y-to-F mutations in the YYD motif substitute for the functional protein. (**F**,**H**,**J**) Phospho mimics do not rescue the mutant phenotype. Dashed lines indicate medulla layers. The boxed areas are magnified to the right. Scale bars: 20 μm.

In contrast to the first tyrosine, the second tyrosine in the YYD motif is conserved not only in invertebrates but also in vertebrates (Fig. 2A), suggesting that it might be the more important of the two for Gogo function. To test this, we mutated each of the tyrosines separately (GogoFYD, GogoYFD, GogoDYD, GogoYDD, Fig. 2B,G-J). Neither of the single phospho mutants (DYD, YDD) rescues the mutant phenotype, whereas both of the phosphomimetic mutants (FYD, YFD) do. We conclude that both tyrosines in the YYD motif are crucial for Gogo function.

Gogo undergoes phosphorylation in vivo

Our studies on the function of Gogo phosphomimetics strongly suggest that Tyr1019 and Tyr1020 are phosphorylation sites. Interestingly, they rather indicate that the dephosphorylation event is important because the non-phosphorylatable Gogo rescues the *gogo*⁻ mutant phenotype. This raises the question as to whether Gogo is tyrosine phosphorylated in vivo.

In a first step, the tyrosine-specific phosphorylation of Gogo was probed in vivo. For this purpose, myc-tagged Gogo was expressed specifically in the visual system (*GMR-gogo-myc*) and co-immunoprecipitated from larval and pupal brains (24 APF). Phosphorylation of the myc-tagged full-length Gogo is clearly visible (Fig. 3A, supplementary material Fig. S2).

Next, we utilized the *Drosophila* S2 cell line to dissect the phosphorylation of Gogo (Fig. 3B-D). Gogo is tyrosine phosphorylated when expressed in S2 cells (Fig. 3C). However, the YYD motif is not the only phosphorylation site (data not shown). The C2 fragment contains nine tyrosines (Fig. 3B) and full-length Gogo with all of them mutated to phenylalanine (Gogo^{9F}) does not show any tyrosine phosphorylation (Fig. 3C). Therefore, the additional potential tyrosine phosphorylation site(s) should be present among them. We restricted our analysis to a short fragment of C2 (amino acids 982-1052, GogoC2^{short}) that covers five tyrosines including the YYD motif and constitutes the most conserved part of the GogoC2 region (Fig. 3B). Using GogoC2^{short} truncation we tested whether the YYD motif is a phosphorylation site. If both tyrosines in the YYD motif are mutated to phenylalanine and the remainder of the tyrosines are intact (GogoC2$^{short\ FFD}$), then the phosphorylation signal is abolished (Fig. 3D), indicating that only the FFD motif is tyrosine phosphorylated in the C2^{short} fragment. However, when each tyrosine residue in the YYD motif is mutated separately (GogoC2$^{short\ FYD}$, GogoC2$^{short\ YFD}$), phosphorylation of the non-mutated amino acid occurs (Fig. 3D). Thus, both Tyr1019 and Tyr1020 are phosphorylation sites.

To confirm that the YYD motif is phosphorylated in the fly, we raised an antibody that specifically recognizes the phosphorylated YYD motif (supplementary material Fig. S3). Although the antibody gives some nonspecific signal, it recognizes wild-type Gogo isolated from the pupal visual system (24 APF) much more strongly than GogoFFD, strongly suggesting that the YYD residues are phosphorylated (Fig. 3F,G).

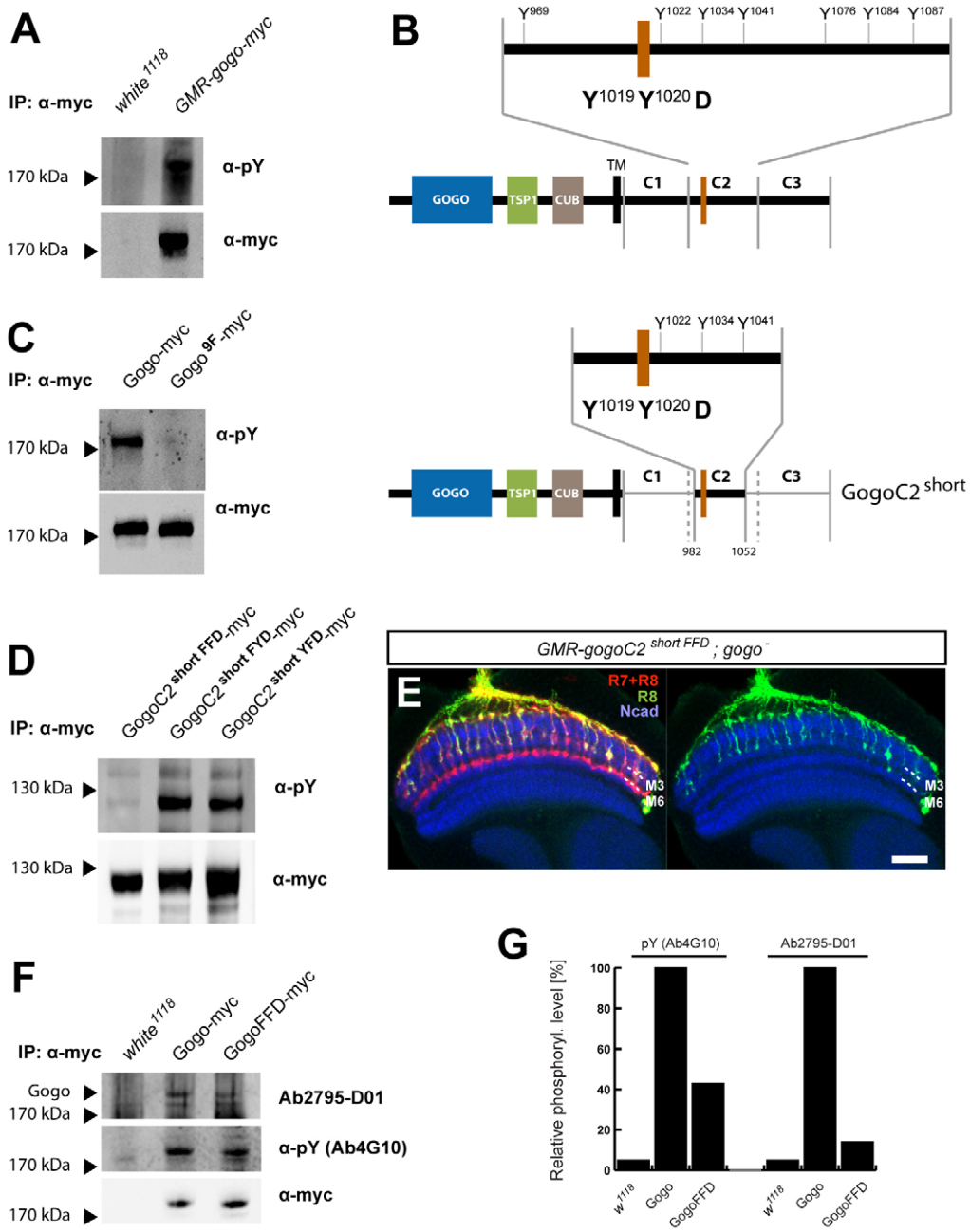

Fig. 3. The YYD motif is phosphorylated in vivo. (**A**) Gogo isolated from pupal photoreceptors (24 APF) is tyrosine phosphorylated (pY). (**B**) The C2 section of Gogo contains nine tyrosines including the YYD motif (Y1019-Y1020-D); the GogoC2^{short} truncation contains only five of them. (**C**) *UAS-gogo-myc* or *UAS-gogo^{9F}-myc* (all nine tyrosines in the C2 section mutated to phenylalanine) was tested for tyrosine phosphorylation in S2 cells. Y-to-F mutations prevent phosphorylation, indicating that Gogo has tyrosine phosphorylation sites in the C2 fragment. (**D**) Both tyrosines in the YYD motif are phosphorylation sites. Mutations in both sites suppress phosphorylation of the GogoC2^{short} truncation (Gogo$^{short\ FFD}$), whereas single-tyrosine mutants (Gogo$^{short\ FYD}$, Gogo$^{short\ YFD}$) show a clear tyrosine phosphorylation signal. (**E**) *GMR-gogo$^{C2\ short\ FFD}$* Dashed lines indicate medulla layers. Scale bar: 20 μm. (**F**) Gogo-myc and GogoFFD-myc expressed in the visual system (*GMR* driver) are tyrosine phosphorylated. A clear quantitative difference in phosphorylation is visible when the phospho-YYD-specific antibody, Ab2795-D01, is used. Pupal brains at 24 APF were dissected for each genotype (n=20 brains). (**G**) Quantification of the western blot in F.

GMR-gogoC2$^{short\ FFD}$ rescues most of the features typical for *gogo*$^{-}$ when expressed in the mutant background: the medulla rotation is completely rescued and the R8 targeting phenotype is partially rescued (70% of R8 neurons target properly, n=372; Fig. 3E). Thus, Tyr1019 and Tyr1020 (the YYD motif) are key phosphorylation sites for Gogo function, whereas the additional potential tyrosine phosphorylation site(s) outside of YYD are not essential.

The YYD motif plays a role in M1 layer recognition

When Gogo (*GMR-Gal4*, *UAS-gogo*) is overexpressed in a wild-type background, R8 photoreceptors exhibit blob-like structures at the medulla M1 layer (Fig. 4A). Based on this and other observations, Gogo was proposed to have an adhesive function at the M1 layer during the early pupal stages, when the R8 axons

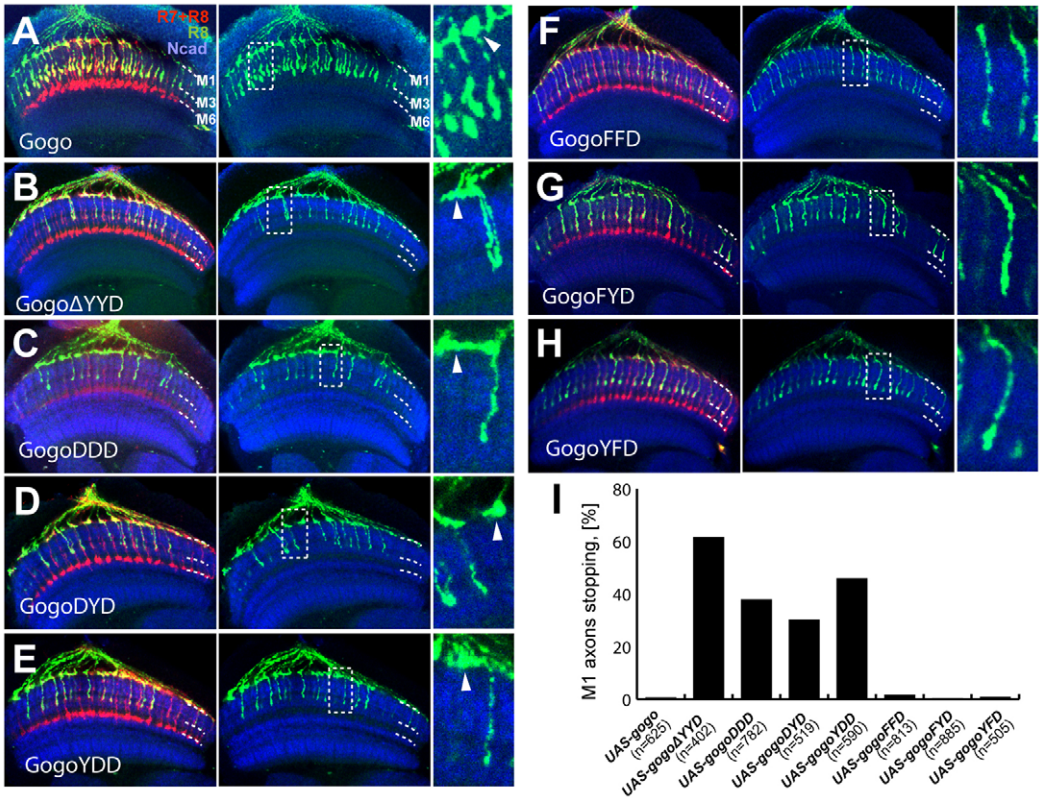

Fig. 4. The YYD motif plays a role in the interaction of R8 axons with the M1 layer. (**A**) Overexpression of wild-type Gogo results in the formation of blobs at the medulla surface (arrowhead). (**B-E**) Removing the YYD motif (B) or mimicking phosphorylation (C-E) results in R8 axons stopping at the temporary layer. Arrowheads indicate premature axon stopping. (**F-H**) Overexpression of non-phosphorylatable Gogo forms does not affect R8 axon targeting. (A-H) Expression of *UAS-gogo* constructs driven by *GMR-Gal4*. Dashed lines indicate medulla layers. The boxed areas are magnified to the right. (**I**) Quantification of R8 axons stopping at the M1 layer.

make a temporal stop at the medulla surface (Tomasi et al., 2008; Hakeda-Suzuki et al., 2011). To determine if YYD tripeptide phosphorylation plays a role in M1 layer recognition, we examined whether mutations in the YYD motif interfere with M1 layer targeting. Because of the specific overexpression phenotype of Gogo, a gain-of-function experiment was suitable to test this (Fig. 4B-I).

To ensure that the observed phenotypes are not caused by differences in expression levels between insertions, the transgenes were inserted into the same locus (supplementary material Fig. S1E-H). Much to our surprise, the overexpression of GogoΔYYD (*GMR-Gal4*) in a wild-type background leads to R8 axons stopping at the M1 layer (Fig. 4B,I). By contrast, the stopping never occurs when wild-type Gogo is overexpressed. The R7 targeting is normal, as deduced from the Mab24B10 staining. The stopping phenotype strongly suggests that the ΔYYD mutation affects the interaction of R8 axons with the temporary targeting of layer M1 during the mid-pupal stage. It indicates that the YYD motif is required to allow R8 photoreceptor axons to leave the M1 layer and proceed to final targeting (M3). If this function of Gogo is blocked (GogoΔYYD), R8 axons fail to innervate the deeper medulla layers.

Since the YYD motif is essential for the interaction with the M1 layer, we speculated that the function of the YYD motif could depend on its phosphorylation state. To test this, we overexpressed *gogo* phospho mutants (Fig. 4C-I). Phospho-Gogo (DDD) showed a similar M1 stopping phenotype to the inactive GogoΔYYD, whereas non-phosphorylatable GogoFFD did not show any obvious mutant phenotype and the targeting was as in wild type (Fig. 4C,F,I). In line with this result, substitution of only one of the tyrosines with a phospho amino acid (DYD, YDD), but not with one that is non-phosphorylatable (FYD, YFD), causes R8 stopping at the M1 layer (Fig. 4D,E,G-I). Combined with our previous result that Gogo is phosphorylated in photoreceptor cells, this suggests that Gogo is phosphorylated at the early stages of development. After the M1 targeting is finalized, Gogo dephosphorylation could permit the R8 axon to leave the M1 layer and target the M3 layer.

In summary, the YYD tripeptide plays an essential role during temporary layer targeting. Deleting the YYD motif or mimicking phosphorylation is sufficient to stop the targeting of R8 photoreceptors at the temporary targeting stage.

The YYD motif and Fmi in M3 layer targeting

We showed previously that Gogo and Fmi act together in R8 axons to recognize and adhere to the M3 layer, as *gogo* and *fmi* co-overexpression in R7 cells induces their mistargeting to the R8 recipient layer (M3), whereas mistargeting never occurs when *gogo* or *fmi* is overexpressed alone (Fig. 5A-C) (Hakeda-Suzuki et al., 2011). Does this interaction also depend on the Gogo phosphorylation status? We analyzed the phenotypes that result when Gogo phospho variants are overexpressed together with Fmi in a wild-type background (Fig. 5D,E). Half of the R7 axons could be redirected to the M3 layer when Fmi was overexpressed together with wild-type Gogo or GogoFFD mimic (Gogo with Fmi, 50% of axons redirected, n=196 axons; GogoFFD with Fmi, 51% of axons redirected, n=406; Fig. 5C,D,F). By contrast, we did not observe an R7 phenotype when Fmi was overexpressed together with GogoDDD (0%, n=380; Fig. 5E,F).

These findings indicate that the Gogo-Fmi interaction required to recognize and adhere to the M3 layer strongly depends on the YYD motif and occurs only when Gogo is dephosphorylated.

DInR regulates Gogo phosphorylation in vivo

DInR has a tyrosine kinase activity and has been shown to be required for photoreceptor axon targeting (Song et al., 2003). Since *dinr* expression is enriched in R-cell projections (Song et al., 2003), it is a candidate modulator of Gogo phosphorylation. To investigate

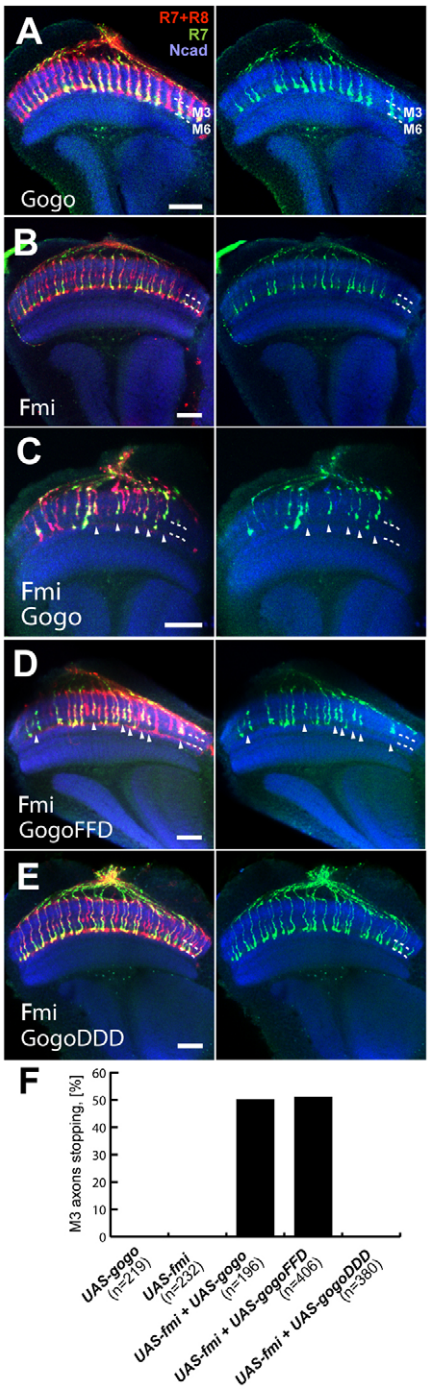

Fig. 5. The Gogo and Fmi interaction necessary to recognize the M3 layer requires Gogo dephosphorylation. (**A**,**B**) When Gogo or Fmi are overexpressed alone the R7 photoreceptors target normally. (**C-E**) Overexpression of Fmi in combination with Gogo (C) or non-phospho-Gogo (D), but not GogoDDD (E), results in R7 axons stopping at the M3 layer. Arrowheads indicate premature R7 axon stopping. Dashed lines indicate medulla layers. Scale bars: 20 μm. (**F**) Quantification of the R7 photoreceptor stopping phenotype.

whether DInR can influence Gogo phosphorylation, we examined the phosphorylation of Gogo co-overexpressed with DInR in S2 cells. Tyrosine phosphorylation, albeit low level, is detected when Gogo is expressed alone (Fig. 6A). Gogo phosphorylation increases dramatically when DInR is co-overexpressed. Moreover, the positive effect of DInR on Gogo phosphorylation is dose dependent (Fig. 6A). This suggests that DInR activity might be required for positive regulation of Gogo phosphorylation and thereby Gogo function.

Does DInR specifically regulate phosphorylation of the YYD motif? To verify this, we modified the Gogo^{short} construct in such a way that the YYD motif is intact but other tyrosines on the cytoplasmic site are mutated (Y1022F, Y1034F, Y1041F). We named this construct Gogo$^{short\ YYD\ FFF}$ (Fig. 6B). Thus, we can be sure that the detected phosphorylation comes only from the YYD motif. The Gogo$^{short\ YYD\ FFF}$ deletion shows a basal phosphorylation, which increases dramatically when DInR is co-expressed (Fig. 6B). We conclude that YYD tripeptide phosphorylation is regulated by DInR activity.

In the *Drosophila* genome there are seven DILPs that could be ligands for DInR. DILPs are evolutionary conserved and act redundantly (Gronke et al., 2010). It has been reported that DInR signaling can be activated by human insulin (Fernandez et al., 1995). To further confirm that DInR signaling modulates Gogo phosphorylation, S2 cells were transfected with Gogo and treated with human insulin for 20 hours. Consistent with the above result, Gogo phosphorylation is enhanced by insulin treatment and insulin-triggered phosphorylation induction is dose dependent (Fig. 6C).

Taken together, these results suggest that the Gogo YYD motif becomes tyrosine phosphorylated upon DInR activation.

dinr and *gogo* interact genetically in photoreceptor axon targeting

Since DInR positively regulates Gogo phosphorylation in S2 cells and phosphorylated Gogo causes R8 photoreceptor stopping at the M1 layer, this raises the possibility that DInR might influence M1 layer targeting by enhancing Gogo phosphorylation. Is it possible to genetically manipulate Gogo phosphorylation by utilizing *dinr*?

To test the *gogo-dinr* genetic interaction, we again took advantage of the *gogo* gain-of-function phenotype (M1 blob). Since GogoDDD does not allow the R8 axons to target the M3 layer and induces stopping on the medulla surface, the increase in Gogo phosphorylation upon DInR overexpression should also affect M1 targeting. Interestingly, although *dinr* shows no gain-of-function phenotype in R8 cells when overexpressed alone (*GMR-Gal4, UAS-dinr*), it strongly enhances the *gogo* gain-of-function phenotype when co-overexpressed (Fig. 6D-F). Quantification showed that when *gogo* is overexpressed alone most of the R8 blobs have an area of no more than 10 μm^2 (92.7% of blobs) and only small numbers of axons form blobs larger than 10 μm^2 (7.2%, Fig. 6G). However, when *dinr* is co-overexpressed with *gogo* the blob size increases dramatically and the proportion of blobs larger than 10 μm^2 increases fourfold (from 7.2% to 31.9%). Furthermore, single axons stopping at the M1 layer or terminating before reaching the M3 layer are visible.

Together, this demonstrates that *dinr* interacts genetically with *gogo* and is able to enhance the phenotype associated with Gogo phosphorylation (stronger adhesiveness to the M1 layer).

dinr and *gogo* interaction requires DInR kinase activity

Since DInR enhances Gogo phosphorylation when co-overexpressed in S2 cells and *dinr* enhances the *gogo* gain-of-function phenotype, it is intriguing whether the *gogo-dinr* interaction requires DInR kinase activity. If the interaction is kinase activity dependent, it would support the model that DInR positively regulates Gogo phosphorylation directly or indirectly. To assess the

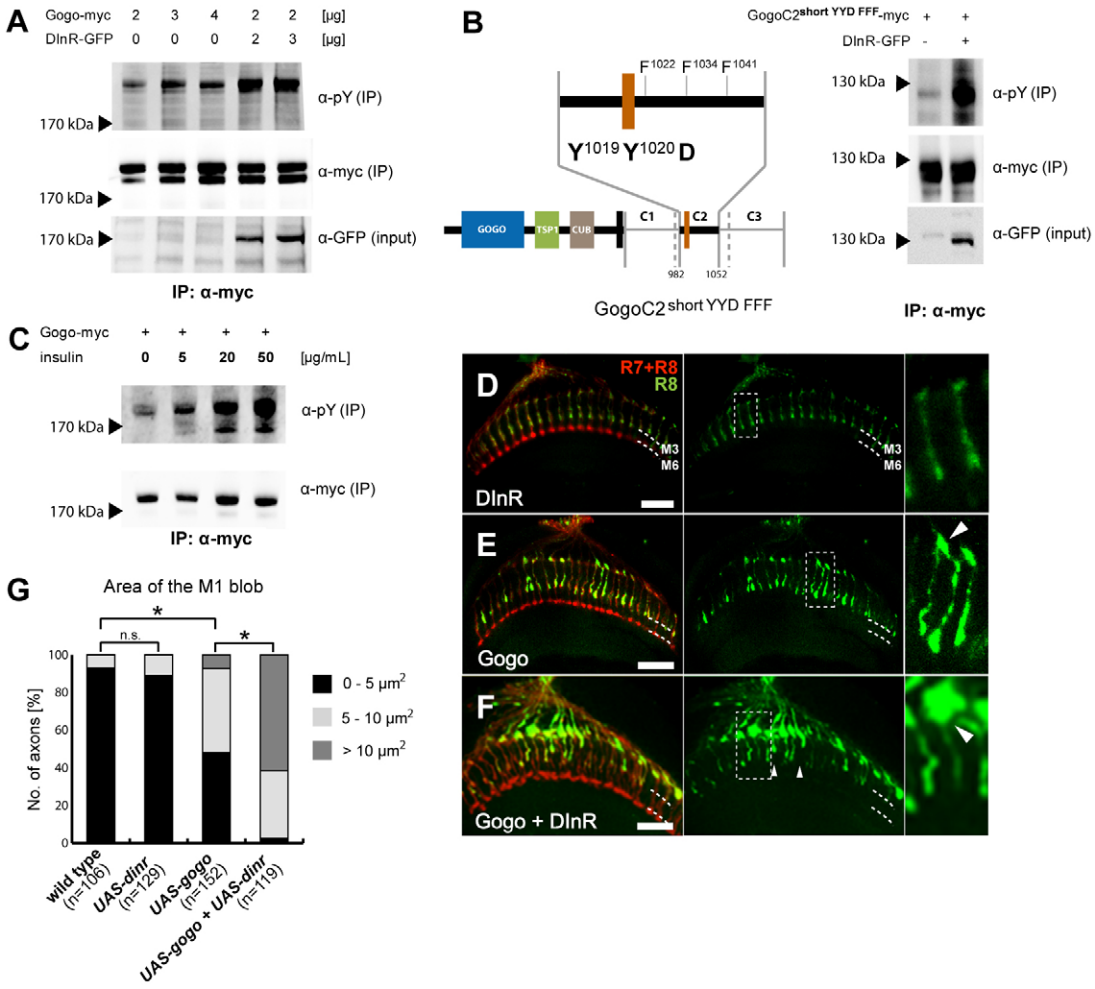

Fig. 6. DInR positively regulates Gogo phosphorylation during R8 targeting. (**A-C**) DInR signaling positively regulates Gogo YYD motif phosphorylation in S2 cells. (A) DInR enhances Gogo phosphorylation in a dose-dependent manner. The indicated amounts of plasmid DNA were used for S2 cell transfection. (B) DInR regulates YYD motif phosphorylation. In the *UAS-gogo*$^{short\ YYD\ FFF}$ construct, only the two tyrosines in the YYD motif are intact, whereas the other three are mutated to phenylalanine (left). The pY signal on the YYD motif is increased upon cotransfection with *dinr* (right). (C) Gogo phosphorylation increases when insulin signaling is stimulated with human insulin (applied for 20 hours at the indicated concentration). (**D-F**) *dinr* interacts genetically with *gogo* during R8 development. (D) *dinr* does not affect photoreceptor targeting when overexpressed in the eye. (E) Overexpression of Gogo results in M1 blob formation (arrowhead). (F) When Gogo and DInR are co-overexpressed, giant blobs are formed at the M1 layer and premature axon stopping is visible (arrowhead). Dashed lines indicate medulla layers. The boxed areas are magnified to the right. Scale bars: 20 µm. (**G**) Quantification of the M1 blob phenotype (*P<0.001, two-tailed t-test). The blobs areas were classified into three categories: 0-5 µm^2, 5-10 µm^2 and greater than 10 µm^2.

DInR kinase activity requirement, we took advantage of available mutant *dinr* transgenic flies that show impaired or enhanced enzymatic activity.

If *gogo* activity is regulated by *dinr* and if phosphorylation of Gogo explains the *gogo* overexpression phenotype, then blob formation should be significantly suppressed if DInR kinase activity is blocked. In order to assess the effect of DInR that lacks its enzymatic activity on Gogo, we utilized the dominant-negative *dinr* fly stock (DInR^{DN}); the K1409A substitution in the kinase domain of DInR^{DN} results in a dominant-negative protein variant (Wu et al., 2005). DInR^{DN} does not show any obvious mutant phenotype when overexpressed alone in all photoreceptors (*GMR-Gal4*, *UAS-dinr*^{DN} Fig. 7A). Moreover, when co-overexpressed with Gogo it can completely suppress blob formation at the M1 layer, indicating that DInR activity is required for blob formation and that it might influence adhesion to the M1 layer during pupal development (Fig. 7B).

We also tested the influence of the constitutively active form of DInR (DInR^{Act}) on the *gogo* overexpression phenotype. The A1325D amino acid substitution in DInR^{Act} mimics the human V938D protein variant (Longo et al., 1992). DInR^{Act} does not have any mutant phenotype when overexpressed alone in a wild-type background (Fig. 7C). A possible reason for this is that the endogenous levels of Gogo are not sufficient to evoke blob formation at the M1 layer, even if most of the Gogo protein undergoes phosphorylation. However, when *gogo* is co-overexpressed with DInR^{Act}, blob formation is enhanced compared with the situation when *gogo* is overexpressed alone, as almost all R8 axons form blobs (Fig. 7D). Additionally, many of the R8 axons fail to target the M3 layer and terminate before reaching their final destination, the M3 layer (7%, n=659). Strikingly, a number of axons even stop at the medulla M1 layer (3%, n=659).

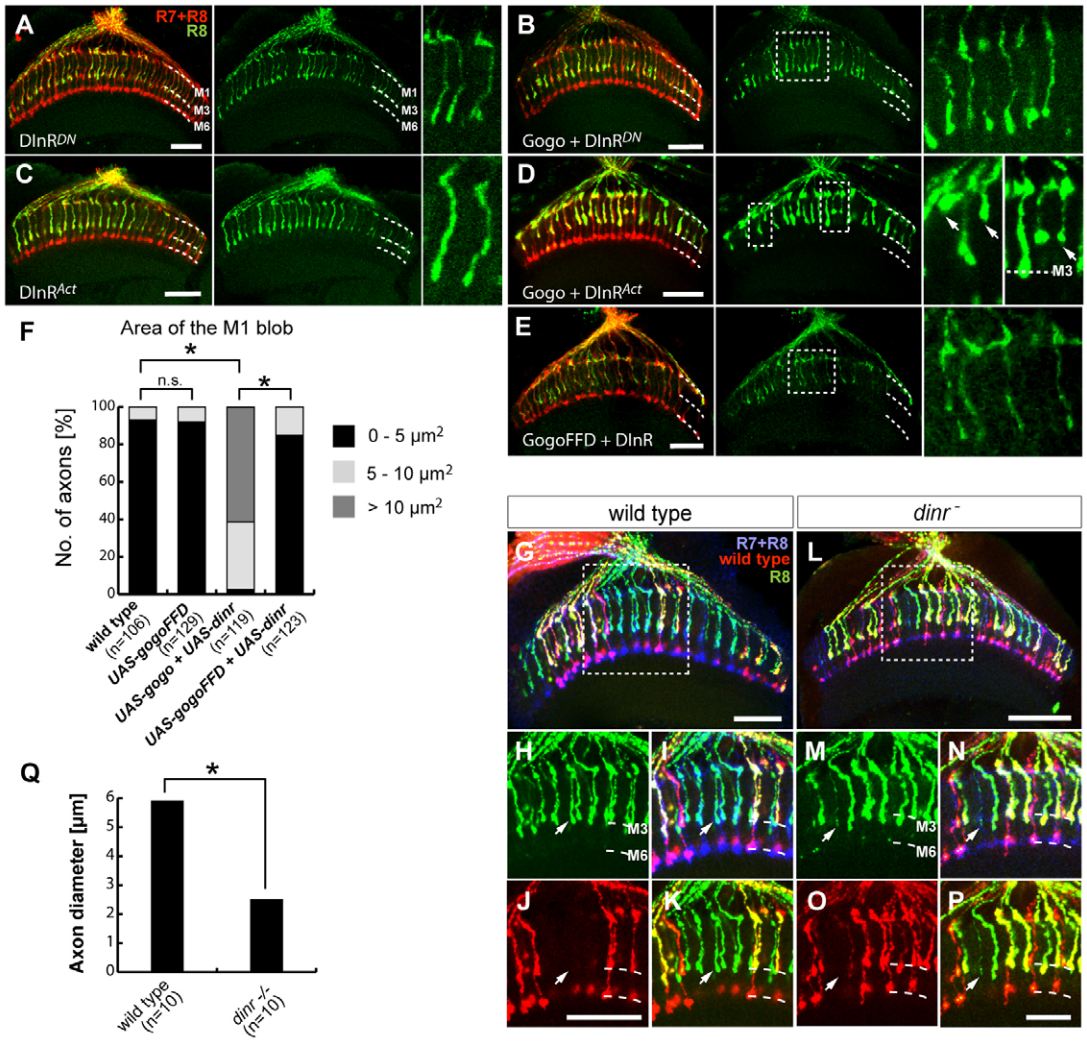

Fig. 7. DInR enzymatic activity is required for potentiating the Gogo overexpression phenotype. (**A**,**B**) DInR^{DN} overexpression in photoreceptors does not affect R8 axon morphology and completely suppresses M1 blob formation when co-overexpressed with Gogo. (**C**,**D**) DInR^{Act} overexpression in photoreceptors does not affect R8 axon morphology and enhances the adhesive properties of R8 axon growth cones when co-overexpressed with Gogo; R8 cells form blobs at the M1 layer and terminate prematurely at M1 or between the M1 and M3 layers (arrows). (A-D) Expression of *UAS* constructs was driven by *GMR-Gal4*. (**E**) DInR does not enhance the *gogo* gain-of-function phenotype when the YYD motif is prevented from being phosphorylated (GogoFFD). (**F**) Quantification of the *dinr-gogo* genetic interaction (*P<0.001, two-tailed *t*-test). Blob area was classified into three categories: 0-5 µm^2, 5-10 µm^2 and greater than 10 µm^2. (**G-P**) R8 axons mutant for *dinr* target the M3 layer normally. Cell patches mutant for *dinr* (*dinr^{ex15}*) were generated in a wild-type background. Wild-type axons express *GMR-KO* (red), and generated clones are negatively labeled by the lack of *GMR-KO* expression (arrow). (G-K) Wild-type R8 axons within the control clone (*FRT82B*) terminate normally at the M3 layer and show normal morphology. (L-P) Axons mutant for *dinr* terminate at the M3 layer and they are abnormally thin. (**Q**) Quantification of axon diameter in *dinr*$^-$ and control R8 projections (*P<0.001, two-tailed *t*-test). Dashed lines indicate medulla layers. The boxed areas are magnified to the right or beneath. Scale bars: 20 µm.

Finally, if DInR modulates Gogo function by positively regulating phosphorylation of the YYD motif, then the enhancement of the *gogo-dinr* co-overexpression phenotype should be suppressed when the YYD motif is mutated to the non-phosphorylatable FFD version. Indeed, blob formation is significantly suppressed and the R8 axon morphology is normal in this situation (Fig. 7E,F).

In a similar approach we co-overexpressed GogoDDD with DInR or DInR^{DN}. In line with the above results, DInR^{DN} does not affect the GogoDDD axon stopping phenotype (supplementary material Fig. S4A,B). DInR slightly increases the GogoDDD axon stopping phenotype; however, this can be explained by the fact that endogenous Gogo is still expressed in the background and can be phosphorylated (supplementary material Fig. S4C).

In summary, the genetic analysis provides evidence that the enzymatic activity of DInR is involved in the interaction with *gogo* and supports the possible involvement of DInR in modulating the phosphorylation status of the Gogo YYD motif and thereby axon pathfinding.

Loss of *dinr* does not affect R8 targeting

It has been reported that DInR functions in axon guidance in the *Drosophila* visual system [R7 photoreceptors (Song et al., 2003)]. In eye-brain complexes of the surviving mosaic larvae (transheterozygous for the hypomorphic alleles *dinr^{353}/dinr^{273}*), R cells failed to expand to their termination points in the medulla. In adult animals (*dinr^{ex15}* null allele clones), gaps in the

R7 layer and crossed fibers were observed (Song et al., 2003). The study by Song et al. does not provide a direct answer as to whether *dinr* also functions in R8 axon guidance because no specific markers for photoreceptor subtypes were used. Thus, we aimed to characterize the function of *dinr* in R8 targeting in more detail by specifically labeling R8 cells that are mutant for *dinr*. We hypothesized that, when *dinr* is inactive, Gogo should be dephosphorylated and the phenotypes observed should resemble the *gogo*$^{-}$ phenotype as rescued by GogoFFD. To determine whether DInR affects axon targeting in the visual system, we used the FLP-FRT system to generate homozygous cell patches mutant for *dinr*^{ex15} in an otherwise wild-type background (Fig. 7G-P).

Although insulin signaling is involved in the regulation of many physiological processes, single photoreceptors mutant for *dinr*^{ex15} survive (Fig. 7L-P). A detailed analysis revealed that all of the analyzed mutant axons have an altered morphology and the axonal process is very thin compared with wild-type axons (on average, 2.5 and 5.9 μm in diameter, respectively, n=10; Fig. 7Q). A possible explanation for this is a crucial role for *dinr* in growth regulation. However, all analyzed R8 photoreceptors target the M3 layer (n=46 axons, 15 brains).

In summary, photoreceptor axons are able to survive upon removal of *dinr* and they do not show any obvious guidance defects; the M3 layer targeting in this case resembles that of the wild type. This is consistent with the result that we obtained when the *gogo*$^{-}$ phenotype is rescued by the non-phosphorylatable GogoFFD.

Endogenous insulin signaling affects R8 axon adhesiveness to the M1 layer

Axons that lack *dinr* target normally. This raises the question of whether endogenous insulin signaling contributes to Gogo phosphorylation. In order to address this issue, we downregulated insulin signaling using two complementary approaches. First, one copy of *dinr* was removed from the fly (*dinr*^{ex15}/+). Second, one copy of *dilp1-5* (five out of seven *dilp* genes in *Drosophila*) was removed (*dilp1-4*^{1}, *5*^{3}/+). In each of these mutant backgrounds Gogo was overexpressed (*UAS-gogo*) and the flies were tested for suppression of the blob phenotype (Fig. 8A-C). In control brains, 30% of R8 axons form blobs at the M1 layer. This phenotype is suppressed when one copy of either *dinr* or *dilp1-5* is removed (*UAS-Gogo; dinr*^{ex15}/+, 12% of axons form blobs; *UAS-Gogo; dilp1-4*^{1}, *5*^{3}/+, 6%; Fig. 8D,E). This suggests that endogenous insulin signaling is involved in Gogo signaling.

DISCUSSION

The YYD tripeptide (Tyr1019-Tyr1020-Asp1021) is conserved among invertebrate and vertebrate species and has a crucial role: deleting it is sufficient to completely abolish Gogo function. YYD is a phosphorylation site and the phosphorylation status of Gogo is critical for both temporary and final layer targeting.

We propose a model in which Gogo is phosphorylated during the first targeting step (0-50 APF). A prolonged phosphorylation during the mid-pupal stage prevents R8 axons from extending to their final layer (Fig. 8F).

Gogo phosphorylation and regulation of R8 axon targeting

Our experiments show that it is the dephosphorylated form of Gogo that is the most active. The non-phospho-Gogo is functional during R8 targeting as we could use it to rescue the *gogo*$^{-}$ mutant phenotype. By contrast, phosphomimetic Gogo does not rescue the mutant phenotype. This mechanism resembles the molecular regulation of Robo activity in that dephosphorylated Robo shows the most activity in mediating repulsive signals during embryonic CNS axon guidance (Bashaw et al., 2000). Additionally, protein inactivation upon phosphorylation, although relatively rare, has been reported in biochemical pathways; for instance, the inactivation of the transcriptional co-activator Yorkie by Warts (Saucedo and Edgar, 2007) and others (Johansen and Ingebritsen, 1986; Lin et al., 1990; Fang et al., 2000).

We were able to abolish Gogo function by removing the YYD site (GogoΔYYD) or by mimicking phosphorylation (GogoDDD). Both forms result in a very strong adhesiveness and in the stopping of growth cones at the M1 layer, suggesting the involvement of phosphorylation in the first targeting step. We postulate that two independent pathways could be activated depending on the phosphorylation status, resulting in either normal M3 layer targeting or M1 stopping, and their activation could be mutually exclusive (supplementary material Fig. S5).

Although dephosphorylated Gogo enables the axons to leave the M1 layer, it is not clear whether in a physiological situation phosphorylation contributes to adhesiveness to the M1 layer. We can say that it might not entirely be necessary, as axons expressing only the dephosphorylated GogoFFD can still recognize the M1 layer (supplementary material Fig. S6). However, there might be more fine-tuning defects, such as in the location of the synapses along the R8 axons between the M1 and M3 layers.

Defects in dephosphorylation can also result in mistargeting of the M3 layer. This is supported by the fact that phospho-Gogo does not show the proper cooperation with Fmi during final layer targeting. Normally, for a proper Gogo-Fmi collaboration, colocalization is required (Hakeda-Suzuki et al., 2011). However, Fmi can colocalize with both phospho- and non-phospho-Gogo, suggesting that the phosphorylation status is important for signal transmission and not for the interaction with Fmi (supplementary material Fig. S7).

Another molecule known to interact with Gogo, Hts (the *Drosophila* homolog of adducin 1) was shown to bind to Gogo and to play a role in guiding photoreceptors (Ohler et al., 2011). However, this physical interaction occurs independently of the YYD site (supplementary material Fig. S8).

gogo and *dinr*

Further evidence for the role of Gogo phosphorylation during R8 targeting comes from the experiments in which we modulated the Gogo phosphorylation status genetically. We searched for kinases and phosphatases that might modulate the Gogo phosphorylation status. The *Drosophila* genome contains a relatively small number of tyrosine kinases (32) and phosphatases (21). We concentrated on proteins that are expressed in the brain, show a transmembrane localization and were implicated in axon guidance. Since Gogo YYD motif phosphorylation is involved in the characteristic overexpression phenotype, it was convenient to screen for the suppression or enhancement of M1 blobs when a kinase or phosphatase was co-overexpressed with *gogo*. From a number of genes tested (*Abl*, *Src42A*, *Src64B*, *drl*, *Egfr*, *dinr*, *Lar*, *Ptp69D*, *eya*) we identified *dinr* as a possible regulator of Gogo phosphorylation. All other tested kinases were excluded from a detailed analysis because the overexpressed genes either did not enhance/suppress the *gogo* gain-of-function phenotype, resulted in extensive cell death, or caused a severe axon guidance phenotype that was difficult to distinguish from a cell death phenotype.

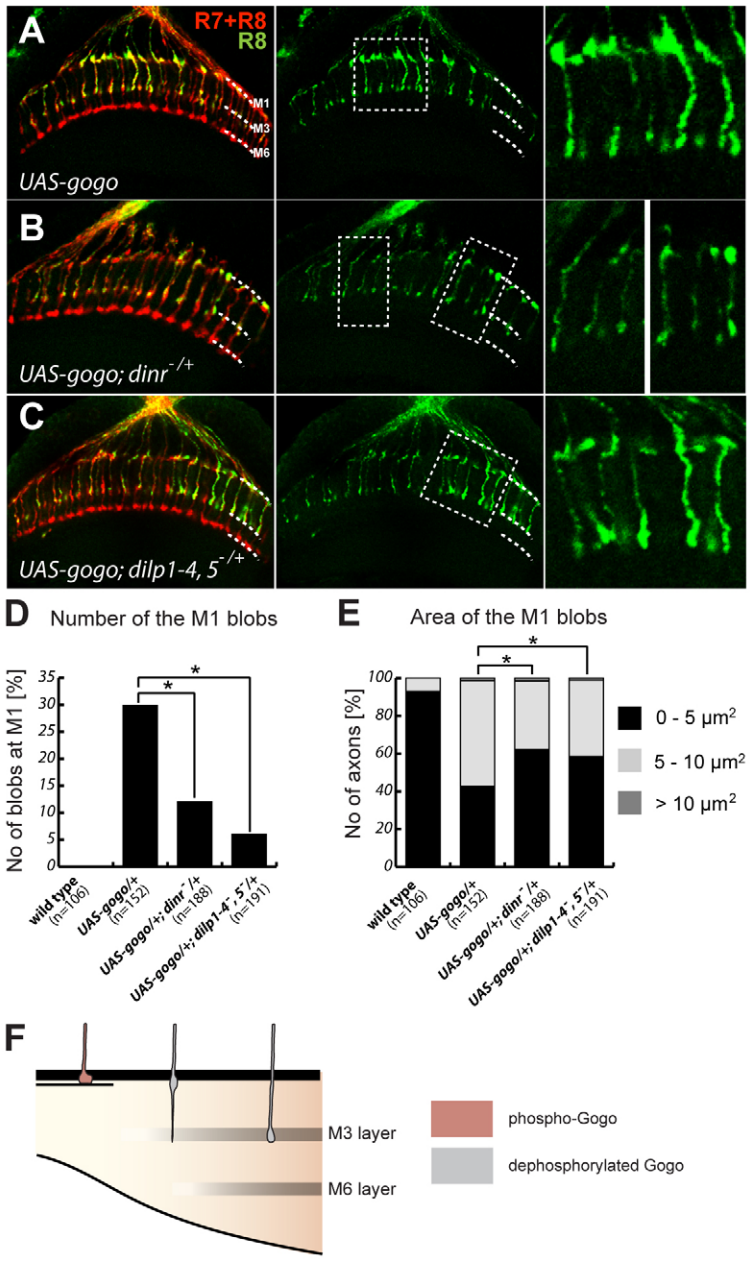

Fig. 8. Endogenous insulin signaling affects R8 axon adhesiveness to the M1 layer. (**A-C**) M1 blob formation upon *gogo* overexpression (A) is suppressed when one copy of *dinr* (B) or *dilp1-5* (C) is removed. Dashed lines indicate medulla layers. The boxed areas are magnified to the right. (**D**,**E**) Quantification of blob phenotype suppression shown in A-C. Both blob number (D) and size (E) are reduced upon insulin signaling downregulation (*P<0.001, two-tailed t-test). (**F**) In our model, Gogo is phosphorylated at the beginning of pupal development (red axons). The phosphorylation must be removed before the R8 process can start targeting to the M3 layer (gray axons).

It is striking that GogoDDD causes a much stronger adhesiveness to the M1 layer than Gogo phosphorylated by overexpressed DInR. A possible explanation is that, unlike GogoDDD, DInR-dependent phosphorylation in this case is not complete. Alternatively, there are redundant mechanisms that further modulate Gogo phosphorylation. Therefore, only a small proportion of photoreceptors stop at the M1 layer and the majority of axons form blob-like structures.

Gogo dephosphorylation as a permissive signal in axon guidance

The cues that a growing axon encounters can be divided into instructive or permissive. Instructive cues usually have a restricted expression pattern and guide the axon by providing either attractive or inhibitory information to the growth cone. Permissive signals steer in response to instructive cues (Bonner and O'Connor, 2001) or are needed to detect and respond to extracellular guidance cues (Dickson, 2001).

Our findings confirm the intriguing possibility that insulin signaling modulates axon guidance (Song et al., 2003). It is difficult to imagine that DInR transduces a typical guidance cue: the only known ligands for DInR, the DILPs, are secreted into the circulatory system (Rulifson et al., 2002) and thus cannot provide a directional cue. Rather, insulin signaling could orchestrate the guidance signals coming from instructive directional cues.

We propose that insulin signaling could be essential for ensuring the correct wiring of the nervous system by influencing the phosphorylation of a regulator of photoreceptor axon guidance, Gogo. Gogo phosphorylation provides a signal that enhances the adhesive interaction with the M1 layer, whereas dephosphorylation could provide a permissive signal that allows the axon to leave the M1 layer and project to the M3 targeting layer.

The state of phosphorylation of a protein at any moment, and thus its activity, depends on the relative activities of the protein kinases and phosphatases that modify it. This suggests that a Gogo dephosphorylation mechanism exists. It would be rewarding to

identify the phosphatase that mediates Gogo dephosphorylation and thereby constitutes an essential regulator of Gogo activity. Our preliminary genetic studies of several candidates, including *Lar* and *Ptp69D*, have not revealed any genetic interaction so far.

In summary, we propose a mechanism whereby the activity of the axon guidance receptor Gogo is regulated by phosphorylation mediated by DInR and dephosphorylation mediated by an as yet unknown phosphatase. This may provide insight into how developmental timing is coordinated in neuronal circuit wiring through a phosphorylation-dephosphorylation mechanism.

Acknowledgements
We thank L. Pick, I. Salecker, L. Partridge, E. Hafen and the Bloomington Stock Center for reagents; I. Grunwald-Kadow and R. Klein for helpful comments; members of the Suzuki laboratory for comments on the manuscript and critical discussion; and M. Sauter for technical assistance.

Funding
This work was supported by the Max Planck Society and a grant from the Deutsche Forschungsgemeinschaft (to T.S.).

Competing interests statement
The authors declare no competing financial interests.

Supplementary material
Supplementary material available online at
http://dev.biologists.org/lookup/suppl/doi:10.1242/dev.074104/-/DC1

References

Alonso, A., Sasin, J., Bottini, N., Friedberg, I., Osterman, A., Godzik, A., Hunter, T., Dixon, J. and Mustelin, T. (2004). Protein tyrosine phosphatases in the human genome. *Cell* **117**, 699-711.
Bashaw, G. J., Kidd, T., Murray, D., Pawson, T. and Goodman, C. S. (2000). Repulsive axon guidance: Abelson and Enabled play opposing roles downstream of the roundabout receptor. *Cell* **101**, 703-715.
Bazigou, E., Apitz, H., Johansson, J., Loren, C. E., Hirst, E. M., Chen, P. L., Palmer, R. H. and Salecker, I. (2007). Anterograde Jelly belly and Alk receptor tyrosine kinase signaling mediates retinal axon targeting in Drosophila. *Cell* **128**, 961-975.
Bischof, J., Maeda, R. K., Hediger, M., Karch, F. and Basler, K. (2007). An optimized transgenesis system for Drosophila using germ-line-specific phiC31 integrases. *Proc. Natl. Acad. Sci. USA* **104**, 3312-3317.
Bonner, J. and O'Connor, T. P. (2001). The permissive cue laminin is essential for growth cone turning in vivo. *J. Neurosci.* **21**, 9782-9791.
Callahan, C. A., Muralidhar, M. G., Lundgren, S. E., Scully, A. L. and Thomas, J. B. (1995). Control of neuronal pathway selection by a Drosophila receptor protein-tyrosine kinase family member. *Nature* **376**, 171-174.
Clandinin, T. R. and Zipursky, S. L. (2002). Making connections in the fly visual system. *Neuron* **35**, 827-841.
Clandinin, T. R., Lee, C. H., Herman, T., Lee, R. C., Yang, A. Y., Ovasapyan, S. and Zipursky, S. L. (2001). Drosophila LAR regulates R1-R6 and R7 target specificity in the visual system. *Neuron* **32**, 237-248.
Dickson, B. J. (2001). Rho GTPases in growth cone guidance. *Curr. Opin. Neurobiol.* **11**, 103-110.
Fang, X., Yu, S. X., Lu, Y., Bast, R. C., Jr, Woodgett, J. R. and Mills, G. B. (2000). Phosphorylation and inactivation of glycogen synthase kinase 3 by protein kinase A. *Proc. Natl. Acad. Sci. USA* **97**, 11960-11965.
Fernandez, R., Tabarini, D., Azpiazu, N., Frasch, M. and Schlessinger, J. (1995). The Drosophila insulin receptor homolog: a gene essential for embryonic development encodes two receptor isoforms with different signaling potential. *EMBO J.* **14**, 3373-3384.
Garrity, P. A., Rao, Y., Salecker, I., McGlade, J., Pawson, T. and Zipursky, S. L. (1996). Drosophila photoreceptor axon guidance and targeting requires the dreadlocks SH2/SH3 adapter protein. *Cell* **85**, 639-650.
Gronke, S., Clarke, D. F., Broughton, S., Andrews, T. D. and Partridge, L. (2010). Molecular evolution and functional characterization of Drosophila insulin-like peptides. *PLoS Genet.* **6**, e1000857.
Hakeda-Suzuki, S., Berger-Muller, S., Tomasi, T., Usui, T., Horiuchi, S. Y., Uemura, T. and Suzuki, T. (2011). Golden Goal collaborates with Flamingo in conferring synaptic-layer specificity in the visual system. *Nat. Neurosci.* **14**, 314-323.
Henkemeyer, M., Orioli, D., Henderson, J. T., Saxton, T. M., Roder, J., Pawson, T. and Klein, R. (1996). Nuk controls pathfinding of commissural axons in the mammalian central nervous system. *Cell* **86**, 35-46.
Hing, H., Xiao, J., Harden, N., Lim, L. and Zipursky, S. L. (1999). Pak functions downstream of Dock to regulate photoreceptor axon guidance in Drosophila. *Cell* **97**, 853-863.
Johansen, J. W. and Ingebritsen, T. S. (1986). Phosphorylation and inactivation of protein phosphatase 1 by pp60v-src. *Proc. Natl. Acad. Sci. USA* **83**, 207-211.
Knoll, B. and Drescher, U. (2004). Src family kinases are involved in EphA receptor-mediated retinal axon guidance. *J. Neurosci.* **24**, 6248-6257.
Lee, R. C., Clandinin, T. R., Lee, C. H., Chen, P. L., Meinertzhagen, I. A. and Zipursky, S. L. (2003). The protocadherin Flamingo is required for axon target selection in the Drosophila visual system. *Nat. Neurosci.* **6**, 557-563.
Lin, A. N., Barnes, S. and Wallace, R. W. (1990). Phosphorylation by protein kinase C inactivates an inositol 1,4,5-trisphosphate 3-kinase purified from human platelets. *Biochem. Biophys. Res. Commun.* **170**, 1371-1376.
Liu, G., Beggs, H., Jurgensen, C., Park, H. T., Tang, H., Gorski, J., Jones, K. R., Reichardt, L. F., Wu, J. and Rao, Y. (2004). Netrin requires focal adhesion kinase and Src family kinases for axon outgrowth and attraction. *Nat. Neurosci.* **7**, 1222-1232.
Longo, N., Shuster, R. C., Griffin, L. D., Langley, S. D. and Elsas, L. J. (1992). Activation of insulin receptor signaling by a single amino acid substitution in the transmembrane domain. *J. Biol. Chem.* **267**, 12416-12419.
Maher, P. A. and Pasquale, E. B. (1988). Tyrosine phosphorylated proteins in different tissues during chick embryo development. *J. Cell Biol.* **106**, 1747-1755.
Maurel-Zaffran, C., Suzuki, T., Gahmon, G., Treisman, J. E. and Dickson, B. J. (2001). Cell-autonomous and -nonautonomous functions of LAR in R7 photoreceptor axon targeting. *Neuron* **32**, 225-235.
Newsome, T. P., Asling, B. and Dickson, B. J. (2000). Analysis of Drosophila photoreceptor axon guidance in eye-specific mosaics. *Development* **127**, 851-860.
Ohler, S., Hakeda-Suzuki, S. and Suzuki, T. (2011). Hts, the Drosophila homologue of Adducin, physically interacts with the transmembrane receptor Golden goal to guide photoreceptor axons. *Dev. Dyn.* **240**, 135-148.
Rulifson, E. J., Kim, S. K. and Nusse, R. (2002). Ablation of insulin-producing neurons in flies: growth and diabetic phenotypes. *Science* **296**, 1118-1120.
Sanes, J. R. and Zipursky, S. L. (2010). Design principles of insect and vertebrate visual systems. *Neuron* **66**, 15-36.
Saucedo, L. J. and Edgar, B. A. (2007). Filling out the Hippo pathway. *Nat. Rev. Mol. Cell Biol.* **8**, 613-621.
Senti, K. A., Usui, T., Boucke, K., Greber, U., Uemura, T. and Dickson, B. J. (2003). Flamingo regulates R8 axon-axon and axon-target interactions in the Drosophila visual system. *Curr. Biol.* **13**, 828-832.
Shinza-Kameda, M., Takasu, E., Sakurai, K., Hayashi, S. and Nose, A. (2006). Regulation of layer-specific targeting by reciprocal expression of a cell adhesion molecule, capricious. *Neuron* **49**, 205-213.
Song, J., Wu, L., Chen, Z., Kohanski, R. A. and Pick, L. (2003). Axons guided by insulin receptor in Drosophila visual system. *Science* **300**, 502-505.
Tarrant, M. K. and Cole, P. A. (2009). The chemical biology of protein phosphorylation. *Annu. Rev. Biochem.* **78**, 797-825.
Ting, C. Y., Yonekura, S., Chung, P., Hsu, S. N., Robertson, H. M., Chiba, A. and Lee, C. H. (2005). Drosophila N-cadherin functions in the first stage of the two-stage layer-selection process of R7 photoreceptor afferents. *Development* **132**, 953-963.
Tomasi, T., Hakeda-Suzuki, S., Ohler, S., Schleiffer, A. and Suzuki, T. (2008). The transmembrane protein Golden goal regulates R8 photoreceptor axon-axon and axon-target interactions. *Neuron* **57**, 691-704.
Wu, J. S. and Luo, L. (2006). A protocol for dissecting Drosophila melanogaster brains for live imaging or immunostaining. *Nat. Protoc.* **1**, 2110-2115.
Wu, Q., Zhang, Y., Xu, J. and Shen, P. (2005). Regulation of hunger-driven behaviors by neural ribosomal S6 kinase in Drosophila. *Proc. Natl. Acad. Sci. USA* **102**, 13289-13294.
Xia, F., Li, J., Hickey, G. W., Tsurumi, A., Larson, K., Guo, D., Yan, S. J., Silver-Morse, L. and Li, W. X. (2008). Raf activation is regulated by tyrosine 510 phosphorylation in Drosophila. *PLoS Biol.* **6**, e128.
Zang, M., Gong, J., Luo, L., Zhou, J., Xiang, X., Huang, W., Huang, Q., Luo, X., Olbrot, M., Peng, Y. et al. (2008). Characterization of Ser338 phosphorylation for Raf-1 activation. *J. Biol. Chem.* **283**, 31429-31437.